Epigenetic assembly of centromeric chromatin at ectopic α-satellite sites on human chromosomes

Megumi Nakano, Yasuhide Okamoto, Jun-ichirou Ohzeki and Hiroshi Masumoto*

Division of Biological Science, Graduate School of Science, Nagoya University, Chikusa-ku, Nagoya 464-8602, Japan

*Author for correspondence (e-mail: g44478a@nucc.cc.nagoya-u.ac.jp)

Accepted 4June 2003
Journal of Cell Science 116, 4021-4034 © 2003 The Company of Biologists Ltd
doi:10.1242/jcs.00697

Summary

To investigate the mechanism of chromatin assembly at human centromeres, we isolated cultured human cell lines in which a transfected alpha-satellite (alphoid) YAC was integrated ectopically into the terminal region of host chromosome 16, where it was stably maintained. Centromere activity of the alphoid YAC was suppressed at ectopic locations on the host chromosome, as indicated by the absent or reduced assembly of CENP-A and -C. However, long-term culture in selective medium, or short-term treatment with the histone deacetylase inhibitor Trichostatin A (TSA), promoted the re-assembly of CENP-A, -B and -C at the YAC site and the release of minichromosomes containing the YAC integration site. Chromatin immunoprecipitation analyses of the re-formed minichromosome and the alphoid YAC-based stable human artificial chromosome both indicated that CENP-A and CENP-B assembled only on the inserted alphoid array but not on the YAC arms. On the YAC arms at the alphoid YAC integration sites, TSA treatment increased both the acetylation level of histone H3 and the transcriptional level of a marker gene. An increase in the level of transcription was also observed after long-term culture in selective medium. These activities, which are associated with changes in chromatin structure, might reverse the suppressed chromatin state of the YAC at ectopic loci, and thus might be involved in the epigenetic change of silent centromeres on ectopic alphoid loci.

Key words: Centromere, Alpha-satellite, Mammalian artificial chromosome, Heterochromatin, Histone acetylation

Introduction

The centromere is an essential functional domain responsible for the correct inheritance of eukaryotic chromosomes during cell division. In mitosis, a specific structure, the kinetochore, is formed at the outer surfaces of the centromere (Brinkley and Stubblefield, 1966; Rattner, 1987; Pluta et al., 1995; Cleveland et al., 2003) and directs chromosome segregation. Several protein components of the centromere/kinetochore structures have been identified, including the centromeric proteins (CENP) CENP-A, -B,-C, -E, -H,-F, and hMis6 (CENP-I) and hMis12 (Warburton, 2001; Goshima et al., 2003; Liu et al., 2003), some of which are conserved between yeast species and humans (Kitagawa and Hieter, 2001). In contrast, centromeric DNA organization varies widely among species (Murphy and Karpen, 1998; Choo, 2001; Henikoff et al., 2001).

Our understanding of the molecular mechanisms that specify the sites of functional centromeres in higher eukaryotes is still incomplete (Shelby et al., 2000). Many observations and analyses of human chromosomes have indicated that the mechanisms specifying the sites for functional centromeres are highly complex. Extensive stretches of alpha satellite (alphoid) DNA, consisting of tandemly repeated, 171 bp units, are present in the centromeric regions of all normal human chromosomes (Willard and Waye, 1987; Choo et al., 1991; Marcais et al., 1993). These sequences colocalize with protein components of the centromere/kinetochore domains (Masumoto et al., 1989a), including CENP-A, a centromere-specific histone H3 variant (Palmer et al., 1991; Sullivan et al., 1994); CENP-B, a CENP-B box (a 17 bp sequence found in alphoid DNA)-binding protein (Earnshaw et al., 1987; Masumoto et al., 1989b; Cooke et al., 1990), and CENP-C, an inner kinetochore protein (Saitoh et al., 1992). However, the presence of alphoid DNA is not sufficient to create a functional centromere structure. On stable dicentric chromosomes, CENP-A, CENP-C and CENP-E [a kinesin-like motor protein found at the kinetochore (Yen et al., 1991; Wood et al., 1997)] do not assemble on the inactive centromere despite the presence of alphoid DNA and CENP-B (Sullivan and Schwartz, 1995; Warburton et al., 1997; Fisher et al., 1997). A marker chromosome containing a neocentromere, which lacks detectable alphoid DNA and CENP-B (du Sart et al., 1997), was found to be mitotically stable, and most of the known centromere proteins assembled at the site of the neocentromere (Saffery et al., 2000). One possible explanation for these phenomena is that centromere activity is maintained by a chromatin assembly mechanism rather than by the primary DNA sequence (Steiner and Clarke, 1994; Williams et al., 1998; Murphy and Karpen, 1998; Wiens and Sorger, 1998).

On all normal human chromosomes, however, functional centromere structures are formed and maintained on alphoid DNA arrays. The mechanisms that specify the location of centromeres are not straightforward, because simple mechanisms do not explain these paradoxical events. Despite these discrepancies, several groups have succeeded in generating mammalian artificial chromosomes (MACs) with functional centromeres that depend on type I alphoid sequences for de novo events (Harrington et al., 1997; Ikeno et al., 1998; Masumoto et al., 1998; Henning et al., 1999; Ebersole et al.,

2000; Mejia et al., 2001; Grimes et al., 2002; Ohzeki et al., 2002). However, MAC formation as the predominant effect was observed in approximately 30-40% of cell lines, and in a subpopulation of cells the multimerized alphoid YAC DNAs integrated into host chromosomes. The different fates of the introduced YAC DNA in different cells suggest that epigenetic controls, such as those that regulate chromatin assembly, are involved in this process.

In this study, to investigate how epigenetic mechanisms direct the assembly of chromatin on human centromeres, we isolated a cell sub-line in which the transfected alphoid YAC DNA was integrated into a host chromosome and was stably maintained without changes in the overall DNA structure of the introduced alphoid YAC array during subcloning. We demonstrate that the suppressed state of centromeres on the alphoid construct can be changed, and that this is accompanied by CENP-A, -B and -C assembly, as shown under two different conditions: long-term culture with selection for the YAC-borne marker, and treatment with an inhibitor of histone deacetylase, Trichostatin A (TSA). Under selective pressure or treatment with TSA the transcription of a marker gene located in the YAC arm was increased. These processes, which change the chromatin structure, might be involved in the mechanisms of epigenetic change of the suppressed state of centromeres at ectopic alphoid DNA loci.

Materials and Methods

Cell lines

The cell lines 7C5HT1, 7C5HT1-2, 7C5HT1-19, 7C5HT2, obtained by α21-I YAC (α7C5hTEL) transfection, and the cell line B13HT1, obtained by α21-II YAC (αB13hTEL) transfection, were described previously (Ikeno et al., 1998). 7C5HT2-1 is a 7C5HT2 derivative. Cell lines del.20HT3-26 and del.22HT1-3 were obtained by transfection of deletion series of the α7C5hTEL YAC, del.20 (30 kb insert of α21-I alphoid) and del.22 (10 kb insert of α21-I alphoid) YAC, respectively, into the cell line HT1080. Details of the characterization of the structure and the capacity for centromere assembly of each deletion of the α21-I alphoid YAC and introduced cell lines will be described elsewhere (Y.O. and H.M., unpublished).

Fluorescence in situ hybridization (FISH)

Standard techniques were employed for FISH (Masumoto et al., 1989a). Probes used were chromosome 16 Painting Probe DIG-labeled (Roche Diagnostics K. K.), p11-4 alphoid DNA (Ikeno et al., 1994) for the α21-I loci and pYAC4 (Burke et al., 1987) for YAC arm DNA. Images were captured using a cooled-CCD camera (PXL, Photometrics Ltd) and analyzed by IPLab software (Signal Analytics).

Indirect immunofluorescence and simultaneous staining by FISH

Indirect immunofluorescence and simultaneous staining by FISH were carried out as previously described (Masumoto et al., 1989a). Antibodies used were anti-CENP-A (mAN1) (Masumoto et al., 1998), anti-CENP-B (2D8D8) (Ohzeki et al., 2002), and anti-CENP-C (CGp2) (Ikeno et al., 1998). In the 7C5HT1-19 and del.22HT1-3 cell lines, more than 50 and 30 metaphase cells from each preparation were analyzed, respectively. Intensities of CENPs and YAC signals on integrated alphoid YACs were analyzed by NIH image (National Institute of Health, USA) and IPLab software (Signal Analytics). Signal intensities with the chromosome 16 painting probe in captured images were measured using IPLab. Each value was normalized to that of the host chromosome 16.

Mitotic stability of re-formed minichromosomes

The cell line 7C5HT1-19 was cultured in selective medium for 60 days and subclones were established during the next 30 days. To test minichromosome stability, the subclones were cultured for a further 60 days in nonselective medium and analyzed by FISH.

Chromatin immunoprecipitation (ChIP)

Cells were crosslinked for 5 minutes in 0.25% formaldehyde. The reaction was stopped by addition of glycine to 417 mM and cells were washed three times with TBS and frozen in liquid nitrogen. Chromatin was fragmented by sonication to a size of 100-500 bp in sonication buffer (5 mM Hepes pH 8.0, 1.5 μM aprotinin, 10 μM leupeptin, 1 mM DTT, 40 μM MG132) using Bioruptor Closed Type Sonicator (Cosmo Bio Co., Ltd).

The soluble chromatin was pre-cleaned with normal mouse IgG (Santa Cruz) and immunoprecipitated with anti-CENP-A (mAN1) or anti-CENP-B (mouse monoclonal antibodies raised against human CENP-B, 2D8D8 and 5E6C1) antibodies in IP buffer (30 mM Hepes pH 8.0, 150 mM NaCl, 1 mM EGTA, 2 mM $MgCl_2$, 2 mM ATP, 1.5 μM aprotinin, 10 μM leupeptin, 1 mM DTT, 0.1% NP-40, 40 μM MG132). Protein G Sepharose (Amersham) blocked with 5% BSA was added, and the antibody-chromatin complex was recovered by centrifugation. The ChIP assay using anti-acetylated histone H3 (Upstate Biotech) was carried out basically according to the manufacturer's protocol. The recovered DNA and the soluble chromatin (as input) were quantitated by real-time PCR. The percentage recovery of DNA fragments and the ratio of enrichment were calculated as described below. The statistical significance of the results obtained was confirmed using the *t*-test (level of significance=0.05).

Real-time PCR

The amount of immunoprecipitated DNA and the dilution of the input DNA were measured by real-time PCR using the iCycler IQ™ Multi-Color Real Time PCR Detection System (Bio-Rad). The following primers were used to amplify *LYS2*, the left alphoid junction, the right alphoid junction, *bsr*, the alphoid 11mer and 5S ribosomal DNA:LYS2-1, 5′-ATGACTAACGAAAAGGTCTGGATA-3′; LYS2-3, 5′-ATCATGAGGCACATCGAGCTGAGG-3′; ARM2, 5′-GCGG-CCGCCCAATGCATTGGTACC-3′; mCbox-3, 5′-AGATTTTAGAT-GATGATATTCCCG-3′; ARM4, 5′-ACCATACCCACGCCGAAAC-AAGCG-3′; mCbox-2, 5′-GCTT(T/G)GAGGATTTCGTTGGAA-GCG-3′; bsr-F, 5′-TCCATTCGAAACTGCACTACCA-3′; bsr-R, 5′-CAGGAGAAATCATTTCGGCAGTAC-3′; 11-10R, 5′-AGGGAA-TGTCTTCCCATAAAAACT-3′; mCbox-4, 5′-GTCTACCTTTTATT-TGAATTCCCG-3′; 5SDNA-F1, 5′-CCGGACCCCAAAGGCGCAC-GCTGG-3′ 5SDNA-R1, 5′-TGGCTGGCGTCTGTGGCACCCGCT-3′. Except for the *bsr* gene, amplifications were carried out using the QuantiTect SYBR Green PCR Kit (QIAGEN). Quantitation of *bsr* was carried out using the Taq-Man probe method with a bsr-FAM probe, the primer 5′-Fam-AATGGCTTCTGCACAAACAGTTACTCGTCC-Tamra-3′ and AmpliTaq Gold DNA polymerase (AP Biosystems).

Trichostatin A treatment of the 7C5HT1-19 cell line

Aliquots of 2.44×10^6 cells were seeded in 10 ml of medium with 250, 500 or 1000 ng/ml of Trichostatin A (TSA) (Wako). After 2 days, the medium was changed. Cell samples for cytological and ChIP analyses were prepared 7 days after removal of the TSA.

Western blot analysis of the TSA-treated 7C5HT1-19 cell line

Extraction of cellular histones was performed basically according to the method of Yoshida et al. (Yoshida et al., 1990). The extracted cellular histones from 5×10^4 cells were applied to a 12% SDS-

polyacrylamide gel or Triton-acid urea gel, electrophoresed, and blotted onto a PVDF membrane (Immobilon, Millipore). The membrane was probed with anti-acetylated histone H3 and H4 (Ac Lys 12) antibodies (Upstate Biotechnology) or anti-CENP-A antibody (mAN1), followed by secondary antibody, anti-rabbit IgG HRP conjugate or anti-mouse IgG HRP conjugate (Bio-Rad). Blots were developed using ECL (Amersham Pharmacia).

RT-PCR and real-time RT-PCR

RT-PCR was carried out using a One-step RNA PCR kit (AMV) (TaKaRa) according to the manufacturer's protocol, using total RNA prepared with the SV Total RNA Isolation system (Promega). Primers for *bsr* amplification were BSR-1 (5′-ATGAAAACATTTAACA-TTTCTCAA-3′) and BSR-4 (5′-TTAATTTCGGGTATATTTGAG-TGG-3′). Primers for human *β-actin* amplification were obtained from Clontech. For each reaction 125 ng of total RNA was used. Products were electrophoresed on agarose gels, and stained with ethidium bromide. Quantitation of transcriptional products was also performed by real-time RT-PCR using the iCycler IQ™ Multi-Color Real Time PCR Detection System (Bio-Rad). Real-time RT-PCR was carried out using a QuantiTect SYBR Green RT-PCR kit (QIAGEN) according to the manufacturer's protocol. Primers for *bsr* amplification were bsr-F and bsr-R. Primers for human *β-actin* amplification were hActin-a (5′-ATCTGGCACCACACCTTCTACAATGAGCTGCG-3′) and hActin-c (5′-GTCATCTTCTCGCGGTTGGCCTTGGGGTTCAG-3′). For each reaction, 20 or 4 ng of total RNA was used. Each quantity of *bsr* transcript was normalized to that of the endogenous *β-actin* transcript, and these ratios compared to that of the 7C5HT1-19 cell line at day 0 (transcription level). Relative copy numbers of the *bsr* gene were quantitated by real-time PCR using genomic DNA. Each transcription level was normalized using the relative copy number of the *bsr* gene (relative transcription). Total RNA from the TSA-treated 7C5HT1-19 cell line was prepared after 2 days of TSA treatment.

Results

Fates of alphoid YAC DNA introduced in a single cell line

Transformation with a YAC (or a BAC) bearing alphoid sequences derived from the centromere of chromosome 21 (α21-I YAC) promoted de novo mammalian artificial chromosome (MAC) formation as the predominant effect in approximately 30% of cell lines. To investigate how epigenetic controls for the chromatin assembly mechanism are involved in centromere/kinetochore formation, we assessed the fate of the introduced alphoid YAC DNA. We subcloned a cell line containing a MAC (7C5HT1) and analyzed derivatives by FISH (Fig. 1A). In one of 19 subcloned cell lines (7C5HT1-19), alphoid YAC DNA signals were detected only in the telomeric region of the short arm of chromosome 16 in every cell examined (Fig. 1A). Restriction analyses of genomic DNA indicated that the overall structure and copy number of the alphoid YAC DNA at the integration site in 7C5HT1-19 cells were not significantly different from those of the original cell line 7C5HT1, which contains a stable MAC (Fig. 1B) [see Fig. 5 in Ikeno et al. (Ikeno et al., 1998)]. Multimerized YACs were stably maintained at the same integration sites in all 7C5HT1-19 cells even after 80 days of culture in nonselective media (Fig. 3A,F bottom). This result suggests that the centromere activity on the integrated alphoid YAC in the 7C5HT1-19 subclone might be functionally suppressed without detectable rearrangement of the multimerized YAC DNA, although we cannot rule out more limited sequence changes.

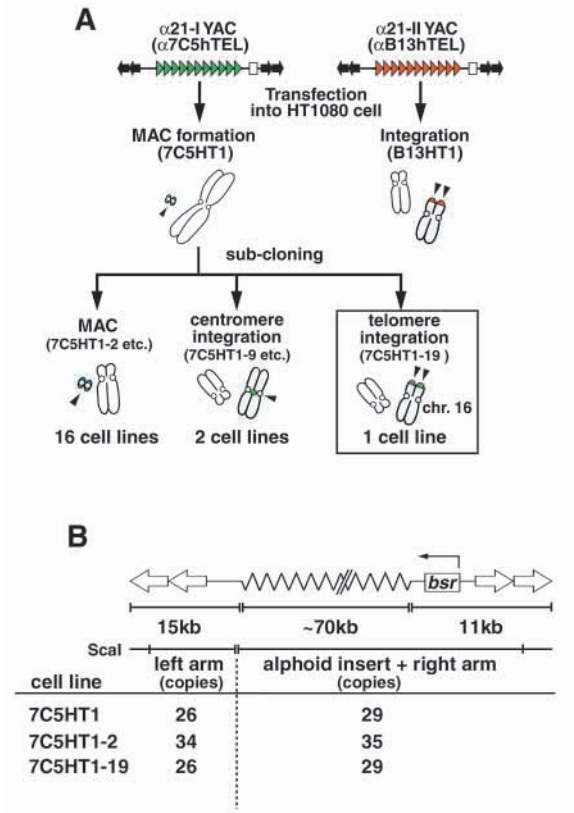

Fig. 1. Cell lines obtained by transfection of an alphoid YAC constructs into HT1080 cells. (A) Following transfection of α21-I alphoid YAC (α7C5hTEL) DNA, the de novo assembly of functional centromeres was observed coincident with MAC formation. MAC formation was not observed for transfection with α21-II alphoid YAC (αB13hTEL). 7C5HT1-19 is a subclone of a MAC-containing cell line (7C5HT1). (B) The structure and copy number of the alphoid YAC in the 7C5HT1 and derivative cell lines were determined by Southern blot analysis (Ikeno et al., 1998; Masumoto et al., 1998).

Disassembly of centromere/kinetochore components at the integration site of alphoid YAC

A chromosome with two functional centromeres (a dicentric chromosome) is mitotically unstable, and can be stabilized by 'inactivation' of one of the two centromeres. At the inactive centromeres of stable dicentric chromosomes, most known centromere proteins are disassembled, although alphoid DNA and CENP-B are still present (Earnshaw and Migeon, 1985). We next examined the assembly of the centromere/kinetochore components CENP-A, CENP-B and CENP-C at the site of integration of the alphoid YAC construct by indirect immunofluorescent staining and simultaneous FISH analysis (Fig. 2A-F). The intensity of each signal relative to that of the native chromosome 16 centromere was measured and plotted (Fig. 2G-L, and for CENP-B also in Fig. 2P). In 17-20% of 7C5HT1-19 cells, CENP-A, -B and -C signals were detected at YAC integration sites (Fig. 2A,C,E,Q, Table 1) but signal intensities were very weak compared with those of the native chromosome 16 centromere (Fig. 2G,I,K). In about 80% of the cells, CENP-A, -B and -C signals were almost undetectable at the YAC integration site, despite the presence of 26-29 copies

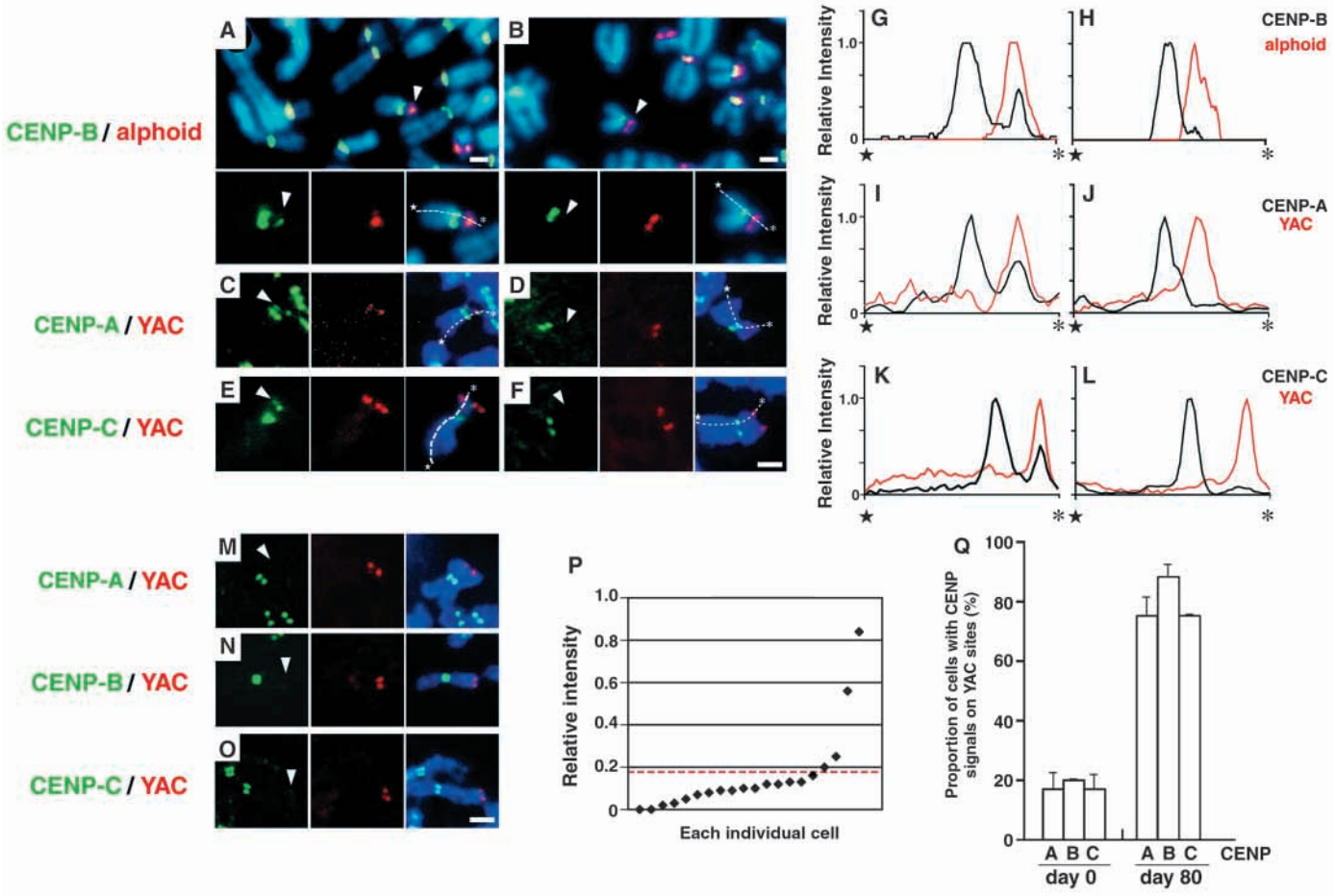

Fig. 2. Assembly and disassembly of CENPs on an integrated alphoid YAC. Metaphase chromosomes from the cell lines 7C5HT1-19 (A-F) and B13HT1 (M-O) were analyzed by FISH with the α21-I probe (red in A,B) or the YAC arm probe (red in C-F,M-O), in combination with immunofluorescence using antibodies against CENPs (green in A-F,M-O). Scale bars: 2 μm. Chromosomes were counterstained with DAPI (blue). Arrowheads indicate the integration sites of the alphoid YAC. (G-L) Plots of the intensity profile of immunofluorescence signals (black) for anti-CENP antibodies and FISH signals (red) along the dotted line on chromosome 16 shown in A-F. Intensities were measured between the positions marked by the star and the asterisk, as shown in merged images of A-F. (P) The intensity of CENP-B immunofluorescence at each alphoid YAC integration site relative to that of the resident centromere on chromosome 16 was plotted. The red dotted line indicates the lower limit of CENP-B signal that is above background level. (Q) The proportion of cells containing the CENPs signals on the alphoid YAC DNA sites. Bars indicate s.e.m. (standard error of mean).

Table 1. Effects of TSA treatment on CENP assembly at alphoid YAC DNA sites

Cell lines	TSA	Percentage of cells with signals for CENPs			Percentage of cells with minichromosomes
		CENP-A	CENP-B	CENP-C	
7C5HT1-19, day 0	–	17 (5.5)	20 (0)	17 (4.9)	0
	+	65	75	54	30 (3.4)
7C5HT1-19 bs+, day 80	–	75 (6.3)	88 (4.2)	75 (0)	58 (2.8)
7C5HT2-1	–	13	39	23	2 (1.4)*
	+	50	60	44	16 (4.9)*
del.20HT3-26	–	nt	nt	nt	2 (1.3)
	+	nt	nt	nt	26*
del.22HT1-3, day 0	–	0	83	0	0
	+	23	91	23	0
B13HT1	–	0	0	0	0
	+	0	0	0	0

Cell lines were treated with 1000 ng/ml (*500 ng/ml) TSA for 2 days and cultured for 7 days without TSA. The percentages of cells with CENP signals and minichromosomes were scored in 25-80 metaphase spreads. 7C5HT1-19 bs+, day 80, is the 7C5HT1-19 subclone cultured for 80 days in selective medium. Values in parentheses are s.e.m. (standard error of mean); nt, not tested.

of the YAC arm fragments and insert alphoid arrays (70 kb) keeping the initial YAC DNA structures (a total length of alphoid arrays corresponds to 2 megabases containing CENP-B binding motif, CENP-B box) (Fig. 1B, Fig. 2B,D,F,H,J,L,Q). These variegated assemblies of CENPs are also observed at synthetic α21-I alphoid BAC integration sites (Ohzeki et al., 2002). In contrast, in the B13HT1 cell line, which was obtained by transfection with the α21-II alphoid YAC and which could not generate active centromeres or MACs, CENP-A, -B, and -C signals specific to the integrated multimerized α21-II DNA were not detected (Fig. 2M-O). These results suggest that the suppressed state of chromatin at the alphoid YAC integration site is stable, similar to what has been observed in inactive centromeres of dicentric chromosomes.

Minichromosome formation associated with an activated centromere on the alphoid YAC site

We used a system containing blasticidin S (BS) and the blasticidin S resistance gene (*bsr*) to obtain alphoid YAC DNA transformants. BS inhibits protein synthesis globally, and the *bsr* gene product inactivates BS by deamination (Dinos and Kalpaxis, 1997). Although introduced alphoid YACs were stably maintained at the same integration sites in all 7C5HT1-19 cells even after 80 days in culture in nonselective medium, when the subclone 7C5HT1-19 was cultured for long periods in medium containing BS the number of YAC integration sites that showed CENP-A, -B and -C signals increased (Fig. 2Q), and a chromosome fragment containing the YAC integration site was frequently observed (Fig. 3A,B). The results of FISH analysis, shown in Fig. 3A, indicate that the proportion of 7C5HT1-19 cells containing a re-formed minichromosome increased with the length of time in culture (from 30% at day 60 to 58% at day 80), while YAC-specific signals decreased at the host chromosome ends (from 64% at day 60 to 32% at day 80). After 80 days of growth in selective medium, 58% of cells contained such a minichromosome signal including the YAC site and 17.1% of cells showed integration of the alphoid YAC at a telomere region of a host chromosome other than chromosome 16. A total of 14.6% of cells still showed the same integration of the alphoid YAC into the chromosome 16 ends by FISH analysis (Fig. 3A,B). Some structural instability and rearrangement involving the exposed double strand breaks might have occurred even in this fibrosarcoma-derived cell line (HT1080) in which a high telomere seeding activity was indicated (Holt et al., 1996; Tsutsui et al., 2003). However, no growth difference was detected between 7C5HT1-2 and 7C5HT1-19. On all the re-formed minichromosomes (100%), CENP-A, -B and -C signals were detected with specific antibodies, along with α21-I YAC signals (Fig. 2Q, Fig. 3D). In addition, the re-formed minichromosomes were very stably maintained as a single extra-chromosomal copy after further culturing for 60 days without the selective drug (Fig. 3E). These results indicate that re-formed minichromosomes contain functional centromere/kinetochore structures. However, in a cell line containing α21-II alphoid YAC DNA (B13HT1), CENP-A, -B, and -C signals were not detected with the multimerized α21-II YAC integration site and chromosome fragments were never released from the integration site under the same conditions (Table 1).

In contrast to the de novo MAC on which no signals derived from host chromosomal fragments were detected (Ikeno et al., 1998; Masumoto et al., 1998; Ohzeki et al., 2002), most re-formed minichromosomes (93%) in 7C5HT1-19 cells contained a small portion of the chromosome 16 arm DNA at various levels (Fig. 3B, middle panel), but with less signal intensity than normal chromosome 16 short arms detected with a chromosome 16 painting probe (Fig. 3C). Thus, in these cases, chromosome breakage might have occurred randomly between the YAC integration site and the native centromere of chromosome 16 (Fig. 3C).

Real-time PCR analysis showed that, although the copy number of alphoid YAC in each cell line changed only 0.8- to 1.2-fold after 80 days in culture, the level of transcription of the *bsr* gene as analyzed by real-time RT-PCR decreased to one tenth the original level after 80 days in culture without selection and increased about threefold under selective conditions (Fig. 3F). Thus, the relative transcriptional level of the *bsr* gene increased during selection, although this transcriptional activity is still very weak compared with that of the endogenous *β-actin* gene. All these results strongly suggest that a functional centromere/kinetochore chromatin structure was re-assembled in parallel with the small increase in the transcriptional activity of the BS resistance gene on the YAC arm through culture under selective conditions.

Direct assembly of CENP-A and -B on introduced α21-I alphoid DNA

To monitor the assembly of CENP-A and CENP-B on introduced alphoid YAC DNA at the molecular level, we carried out chromatin immunoprecipitation (ChIP) assays on 7C5HT1-2 cells, 100% of which contain a single stable MAC (Fig. 1). Cells were fixed with formaldehyde and sonicated to reduce the size of DNA to 100-500 bp, and then immunoprecipitated with mouse monoclonal antibodies against CENP-A or -B. The precipitated DNA samples were quantitated by real-time PCR with the primer sets shown in Fig. 4A. All of the primer pairs could amplify the target sequences in a concentration-dependent manner in real-time PCR using sequential dilutions from 10^{-1} to 10^{-4} of input DNA (Fig. 4B). Immunoprecipitation with all the antibodies tested allowed very low and similar levels of recovery of control 5S ribosomal DNA on which no centromere protein assembly was observed (Ikeno et al., 1998) (Fig. 4C). Therefore, we used the recovery ratios of 5S ribosomal DNA to the input DNA as an internal control for normalization of the recovery ratio of the DNA fragment from each cell line. The relative enrichment of each DNA fragment compared to the recovery of 5S ribosomal DNA by the immunoprecipitation analysis is indicated in Fig. 4D,E,F. By immunoprecipitation with mouse normal IgG, no specific chromatin site was precipitated (Fig. 4D, enrichment ratios are 0.5- to 1.4-fold) in any of the cells tested. α21-I alphoid arrays were specifically and highly enriched 6.7- to 13-fold and 13- to 25-fold by immunoprecipitation with anti-CENP-A and anti-CENP-B antibodies, respectively, in all cell lines analyzed and under all conditions (Fig. 4E,F). This result is consistent with many cytological observations showing centromere protein assembly on α21-I alphoid sequences (Ikeno et al., 1994; Ikeno et al., 1998; Masumoto et al., 1998).

However, in this ChIP analysis, it is difficult to distinguish

α21-I alphoid sequences on introduced YAC DNA from α21-I alphoid DNA at the native centromere of chromosome 21. We have demonstrated de novo assembly of CENP-A on introduced alphoid DNA derived from synthetic (thus distinguishable) α21-I type alphoid using another ChIP and competitive PCR assay (Ohzeki et al., 2002). Thus, in the present study, we designed primers that bridge the boundaries between the insert alphoid DNA and the YAC left or right arm (the left alphoid junction or the right alphoid junction, respectively). Both the left and the right alphoid junctions containing alphoid DNA with the CENP-B box as its principal component were also enriched 4.9- to 6.0-fold and 4.2- to 4.5-fold with anti-CENP-A and anti-CENP-B antibodies, respectively, in 7C5HT1-2 cells, which contain a single stable MAC (Fig. 4E,F). In contrast, the *LYS* locus on the YAC left arm and the *bsr* locus on the right arm were only slightly enriched with these antibodies (0.8- to 1.8-fold). The results indicate that, despite the multimeric structure of the alphoid YAC DNA, CENP-A and CENP-B actually associated only with the 70 kb alphoid arrays on the de novo

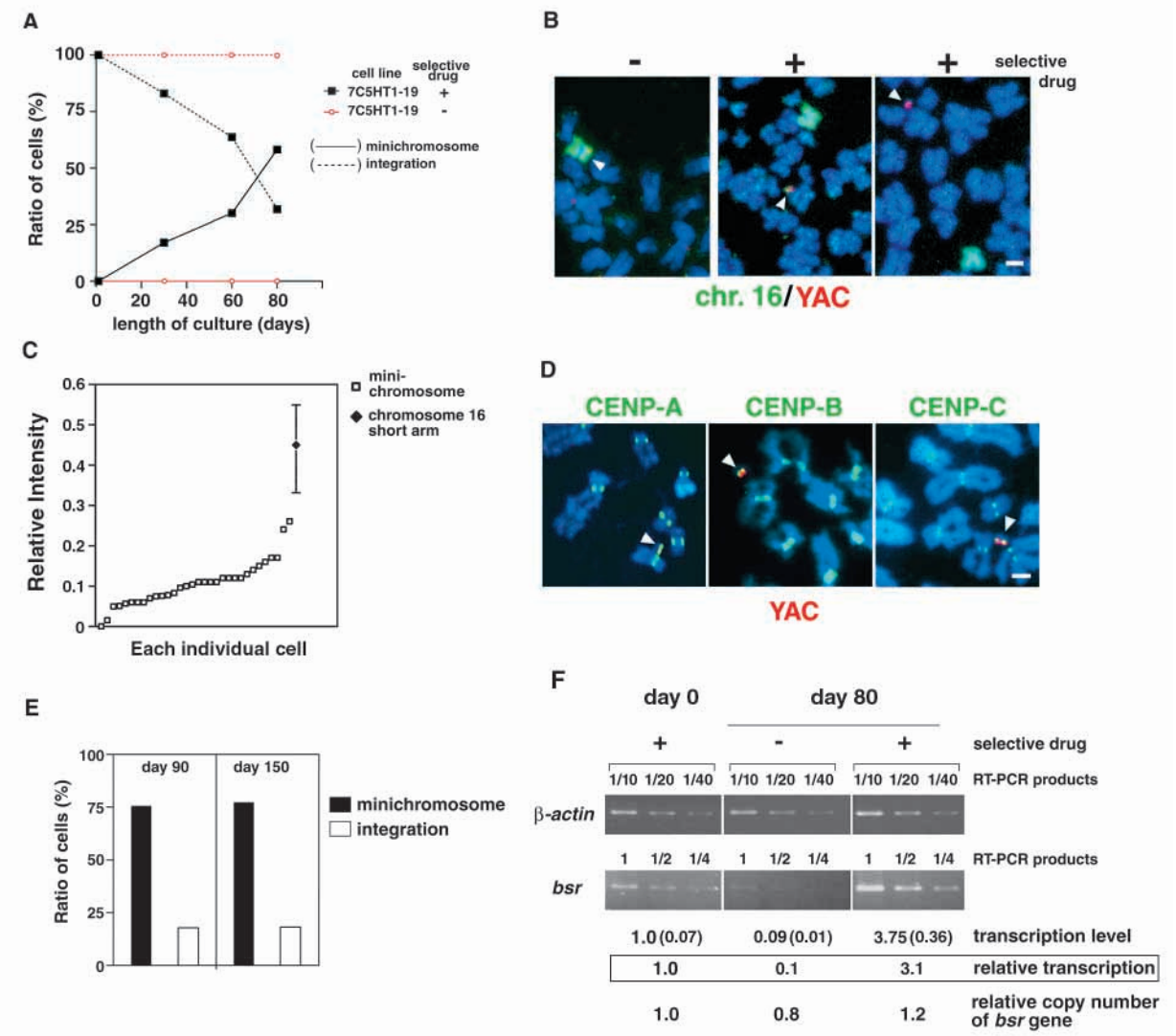

Fig. 3. Minichromosome re-formation in the cell line 7C5HT1-19. (A) The proportion of cells containing minichromosomes (solid line) or the integrated alphoid YAC site (dashed line). 7C5HT1-19 cells were cultured in selective (square) or nonselective (circle) medium for the number of days indicated. More than 50 metaphase cells were analyzed for each observation. (B) 7C5HT1-19 metaphase chromosomes after 80 days in culture in either nonselective (left) or selective (middle and right) medium. FISH probes specific to the whole of human chromosome 16 (green) and to YAC arm sequences (red) were used. Arrowheads indicate alphoid YAC DNA. Scale bar: 2 μm. (C) FISH signal intensities with the chromosome 16 probe on re-formed minichromosomes relative to that of the host chromosome 16. The diamond indicates the average intensity for the short arm of chromosome 16. Bars indicate maximum and minimum values. (D) Assembly of CENPs on re-formed minichromosomes. Indirect immunofluorescence and simultaneous staining by FISH was performed to detect CENPs (green) and the YAC arm (red). Arrowheads indicate minichromosomes. Scale bar: 2 μm. (E) Stability of re-formed minichromosomes in 7C5HT1-19 cells after 60 days in nonselective medium. (F) RT-PCR analysis of *bsr* transcripts. (Upper) Portions of RT-PCR products amplified with primers specific to the *bsr* gene and the human *β-actin* gene (1, 1/2, 1/4 and 1/10, 1/20, 1/40, respectively) were electrophoresed in agarose gel. (lower) Ratios of transcriptional products of *bsr* to those of the 7C5HT1-19 cell line at day 0 quantitated by real-time RT-PCR. Both analyses showed the same transcription levels of *bsr*. The relative copy number of *bsr* genes was quantitated by real-time PCR.

MAC, and CENP-A and CENP-B did not assemble on the YAC arms.

In contrast, in the 7C5HT1-19 cell line, the left and right alphoid junctions were enriched only 1.8- to 2.3-fold with anti-CENP-A and anti-CENP-B antibodies, indicating that CENP-A and CENP-B assembly on the ectopic alphoid array of the integrated YAC was also reduced at molecular level (Fig. 4E,F). However, when 7C5HT1-19 cells were cultured for 80 days with BS selection, both of the alphoid junctions were enriched 3.6- to 9.2-fold by immunoprecipitation with anti-CENP-A and anti-CENP-B antibodies (Fig. 4E,F). The re-assembly of CENP-A and CENP-B, as shown by the ChIP analysis, coincided well with cytological observations of the same cell lines cultured for 80 days with BS selection. All these results indicate that in 7C5HT1-19 cells, the extent of CENP-A and -B assembly on integrated alphoid YAC DNA was reduced, reflecting centromere inactivity, and increased when minichromosome formation was induced by long-term culture with BS selection. However, even under conditions in which a 3.6- to 9.2-fold enrichment of the alphoid junctions was achieved, DNA sequences on both YAC arms (*bsr* and *LYS* sites) were not significantly immunoprecipitated with anti-CENP-A and anti-CENP-B antibodies (1.0- to 2.0-fold), suggesting that epigenetic CENP-A and CENP-B re-assembly remained restricted to the 70 kb α21-I alphoid DNA array (Fig. 4E,F).

Minichromosome formation and CENP re-assembly induced by inhibition of histone deacetylase

What is the mechanism responsible for the re-assembly of centromere components? To study this question, cells showing relatively higher transcription activity of the *bsr* gene were selected by long-term culture with blasticidin S (BS). In treated cells, the chromatin structure might differ from its original state. Therefore, one possible explanation is that during long-

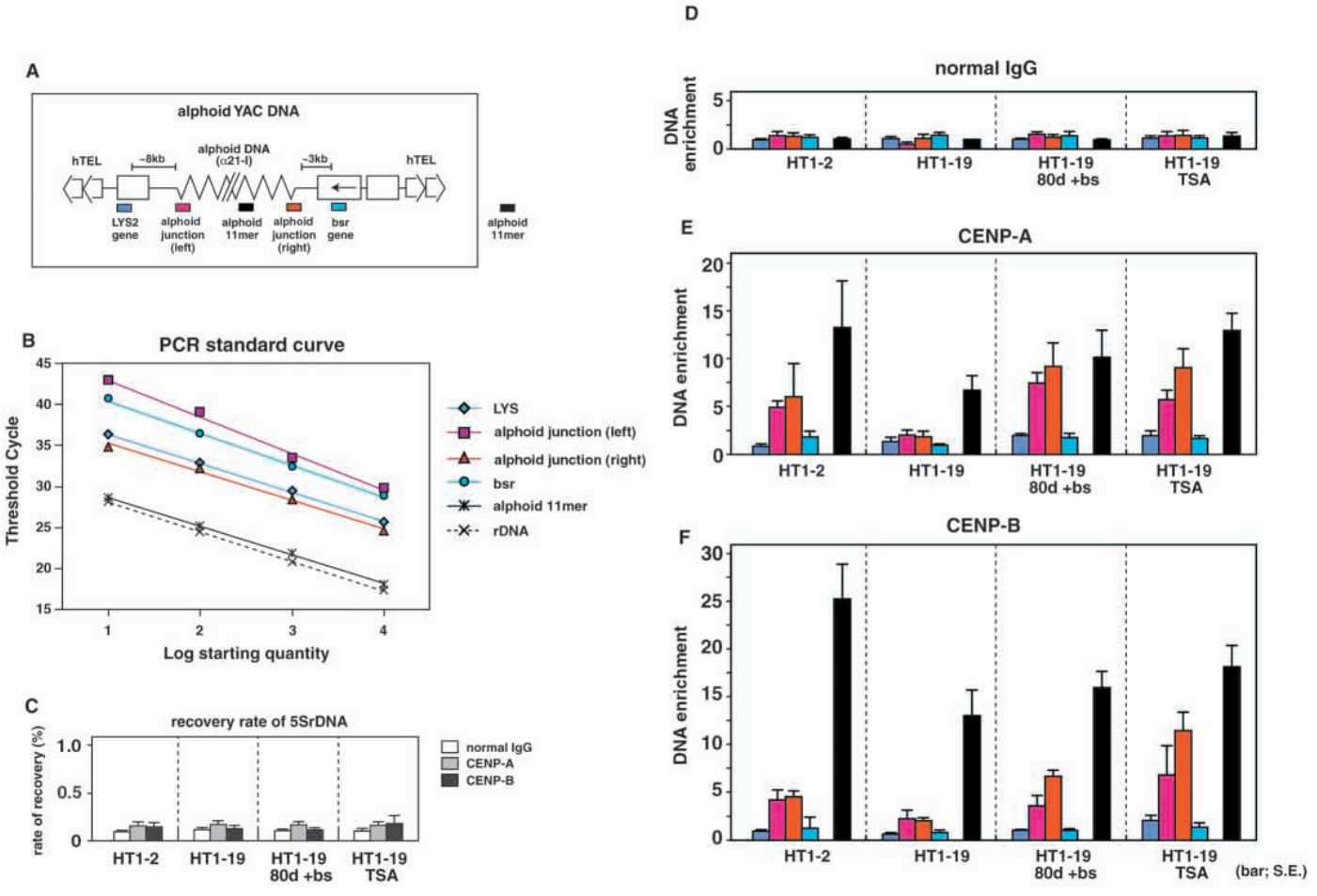

Fig. 4. ChIP analysis of CENP-A and CENP-B on introduced alphoid YAC DNA. (A) Positions of PCR primer pairs on alphoid YAC DNA are indicated. (B) Standard curves of real-time PCR using the primer pairs indicated in A and sequentially diluted input DNAs. All the primer pairs showed a concentration-dependent amplification of the target sequences. (C-F) Fixed and sonicated chromatin from the cell lines indicated was immunoprecipitated with mouse normal IgG, anti-CENP-A antibody, and anti-CENP-B antibody. The immunoprecipitated DNA was quantitated by real-time PCR using the primers indicated in A. (C) The bar charts show the percentage recovery (% IP) of 5S ribosomal DNA fragment by immunoprecipitation using the indicated antibodies. (D-F) The bar charts show the relative enrichment, calculated by dividing the % IP of each DNA region by that of the 5S ribosomal DNA fragment immunoprecipitated by normal mouse IgG (D), anti-CENP-A antibody (E) and anti-CENP-B antibody (F). ChIP analysis was performed four times and the average of the results is presented. The colors of the columns denote the different DNA sequences as shown in A. Bars indicate s.e.m.

term culture in medium containing BS, structural changes in chromatin might have occurred at the ectopic alphoid YAC site that would allow the assembly of functional centromere/kinetochore components. To test this hypothesis, we used a histone deacetylase inhibitor, Trichostatin A (TSA) (Yoshida et al., 1990), to alter the state of chromatin at YAC integration sites. TSA treatment causes histone hyperacetylation and converts a transcriptionally inactive chromatin structure into an active one at many loci (Bartsch et al., 1996). The results of western blotting indicated that the levels of acetylation of histone H3 and H4 in the cell line 7C5HT1-19 were increased by TSA treatment for 2 days (Fig. 5A). In contrast to what was observed for histone H4, using Triton-acid urea (TAU) gel, neither the mobility nor the

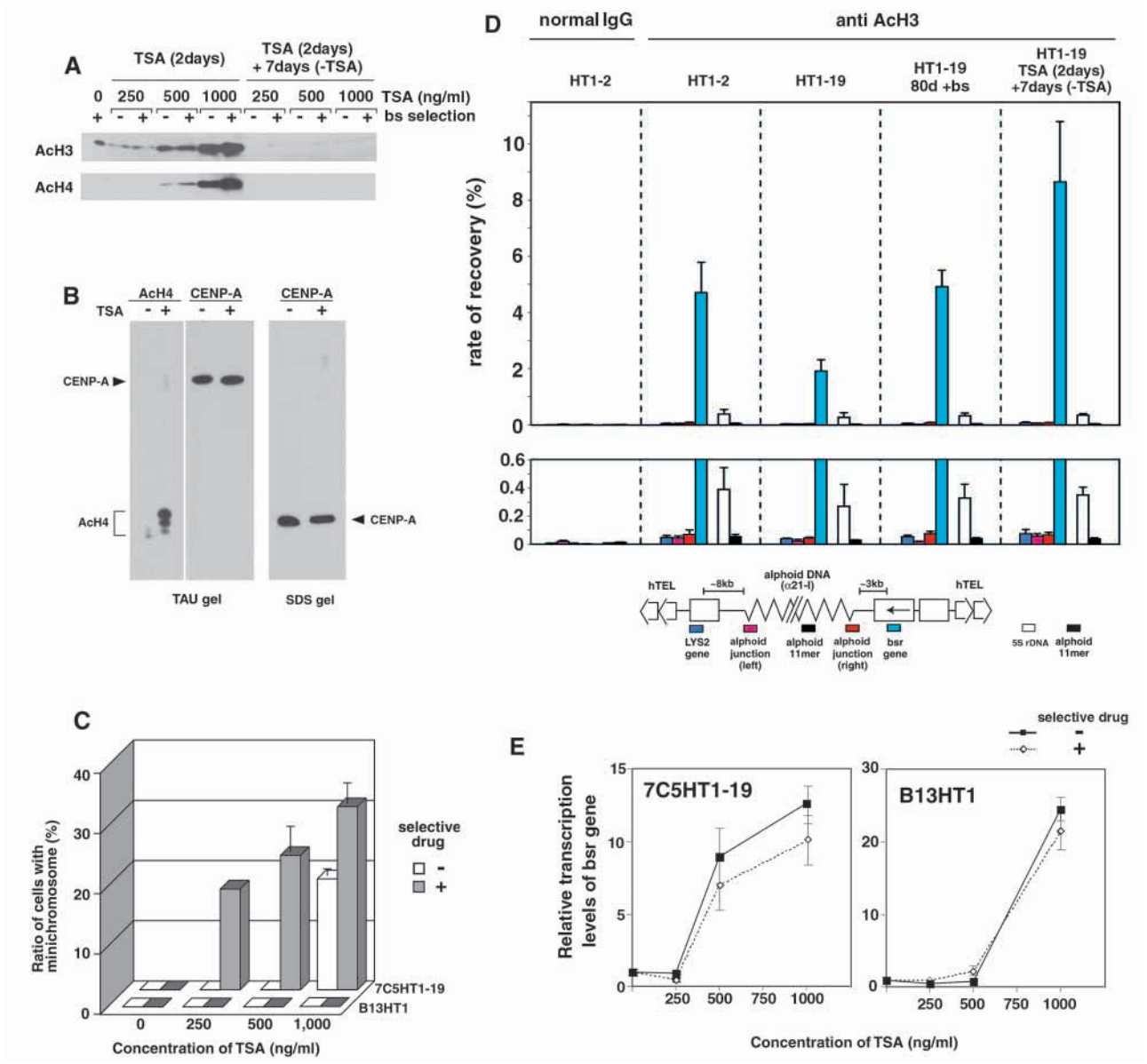

Fig. 5. Effects of TSA treatment on the ectopic alphoid YAC sites. (A) 7C5HT1-19 cells were analyzed after 2 days of TSA treatment or after a further 7 days of culture without TSA, by western blotting using anti-acetylated histone H3 (upper) and H4 (lower) antibodies. (B) 7C5HT1-19 cells were treated with TSA and applied to TAU gel (left and middle) and SDS gel (right) and analyzed by western blotting with anti-acetylated histone H4 (Lys 12) or anti-CENP-A antibody. (C) Proportions of cells containing a minichromosome. Cells were treated with the indicated concentrations of TSA for 2 days and then cultured for 7 days without TSA. More than 50 metaphase cells were analyzed for each sample. Bars indicate s.e.m. (D) ChIP analysis of TSA-treated 7C5HT1-19 cells using anti-acetylated histone H3 antibody. HT1-19 cells were treated with 1 μg/ml of TSA for 2 days and then cultured for 7 days without TSA. Immunoprecipitated DNA was quantitated by real-time PCR using primers indicated in Fig. 4A. The bar chart shows the percentage of recovery by immunoprecipitation (% IP) using normal IgG or anti-acetylated histone H3 antibody. The colors of the columns denote the different DNA sequences as shown in lower panel. Bars indicate s.e.m. (E) Relative transcription levels of the *bsr* gene in TSA-treated cells were analyzed by real-time RT-PCR. The transcription levels of the *β-actin* gene were not significantly changed by the TSA treatment in this analysis, so each level of *bsr* transcript was normalized to that of the *β-actin* transcript. Bars indicate s.e.m.

intensity of CENP-A was affected directly, even by 1000 ng/ml of TSA treatment, in our experiment (Fig. 5B). The effect of TSA treatment on minichromosome re-formation and CENP re-assembly was analyzed after 7 days in culture after removal of TSA, because high concentrations of TSA cause cell cycle arrest in the G1 and G2 phases (data not shown). During this period, the levels of histone H3 and H4 acetylation in 7C5HT1-19 cells were reduced to the levels seen in untreated cells (Fig. 5A). FISH analysis combined with indirect immunofluorescence staining showed that the assembly of centromere proteins at the alphoid YAC sites occurred in 54–75% of 7C5HT1-19 cells cultured after TSA treatment, and minichromosomes with active centromere components also formed in 17–30% of the cells (Fig. 5C, Table 1). Similar results were obtained following treatment with sodium butyrate (data not shown), another histone deacetylase inhibitor (Candido et al., 1978). The ChIP analysis indicated that TSA treatment of 7C5HT1-19 cells caused a 5.7- to 11-fold enrichment of both alphoid junctions on the YAC site by immunoprecipitation with anti-CENP-A and anti-CENP-B antibodies (Fig. 4E,F). However, DNA sequences on both YAC arms (*bsr* and *LYS* sites) were not significantly enriched (1.3- to 2.1-fold). Thus the same phenomenon, indicating epigenetic CENP-A and CENP-B re-assembly and activation of a centromere restricted to the ectopic 70 kb α21-I alphoid DNA array, was produced by two different treatments of the cells: long-term culture with BS selection or short-term culture with TSA.

Centromere activation associated with the activation of transcription of a YAC marker gene

What is the common mechanism by which both treatments affect the ectopic alphoid YAC sites? During long-term culture with BS selection, the relative transcriptional level of the *bsr* gene on the YAC arm increased. We therefore analyzed the effect of TSA on the chromatin structure at the introduced alphoid YAC locus by using a ChIP assay with an antibody against acetylated histone H3 (Fig. 5D). The extent of recovery of alphoid DNA, 5S ribosomal DNA and the sequences of the YAC were assessed in recovered DNA by real-time PCR (e.g. Fig. 4A,B). Acetylated histone H3 assembles anywhere on DNA, so that in this analysis we directly compared each ratio of the recovered DNA to the input DNA. With control normal IgG, all the tested DNA fragments were recovered at low levels (less than 0.014±0.008%, Fig. 5D). The ratio of recovery of *bsr* sequences derived from the YAC vector on the artificial chromosome with an active centromere in 7C5HT1-2 cells was very high (4.7%) with the anti-acetylated histone H3 antibody compared with the recovery of 5S ribosomal DNA (0.39% in Fig. 5D), genomic alphoid DNA (0.054%), the left and the right alphoid junctions (0.044, 0.070%, respectively) and *LYS* locus (0.048%). On the other hand, the ratio of recovery of the *bsr* gene from the YAC integration site in 7C5HT1-19 cells with anti-acetylated histone H3 was low (1.9%, 1/2.5 of that of the *bsr* gene in 7C5HT1-2 cells). However, after TSA treatment recovery increased 4.6-fold (8.7%). In contrast, those of 5S ribosomal DNAs (0.27-0.35%), genomic alphoid, the left and the right alphoid junctions and *LYS* locus (less than 0.075%) were changed by 1.3- to 2.4-fold, with very low levels even after the TSA treatment. After 80 days of culture with BS selection, the ratio of recovery of the *bsr* gene increased to 4.9%, reaching the same level as with artificial chromosomes. The patterns of the recovery of each DNA sequences on the YAC in 7C5HT1-2 cells were similar but increased by 1.2- to 1.6-fold after TSA treatment (data not shown). All these results indicate that histone H3 associated only with the *bsr* locus was hyperacetylated on the artificial chromosome containing the active centromere, on the YAC integration site in cells treated with TSA and on the YAC site in cells after 80 days of the culture with the selective condition. The level of transcription of the *bsr* gene as analyzed by real-time RT-PCR increased with a higher TSA concentration (Fig. 5E). Thus, these results indicate that TSA treatment changes the chromatin structure of the *bsr* gene, which is close to the insert alphoid DNA on the YAC site, into a weak transcription-capable state.

De novo assembly of active centromere/kinetochore components without chromosome rearrangements

We examined several different cell lines (7C5HT2-1, del.20HT3-26) in which α21-I YAC and its derivative YACs and BACs were integrated at other sites. TSA treatment also caused minichromosomes to form at varying frequency, accompanied by CENP-A, -B and -C signals from the α21-I YAC integration sites in these cell lines (Table 1). When the 10 kb α21-I alphoid DNA YAC was integrated at an interstitial site (del.22HT1-3 cell line; about 98 copies of multimerized YAC DNA were integrated into a single site of a host chromosome, thus totaling 980 kb of α21-I alphoid DNA but interrupted by YAC arm sequences about every 10 kb of α21-I alphoid array, data not shown), no assembly of CENP-A and -C was detected on the YAC sites with the specific antibodies (Fig. 6A,E,H,L,N, Table 1). However, TSA treatment induced the de novo assembly of CENP-A and CENP-C at this 10 kb alphoid YAC integration site without chromosome breakage (Fig. 6B,F,I,M,N, Table 1). Even before TSA treatment, CENP-B signals were detected at YAC integration sites in 83% of cells (Fig. 6C,J,N, Table 1); however, of these, 62% showed very weak CENP-B assembly which could barely be distinguished from background levels (Fig. 6N). After TSA treatment, the intensity of the CENP-B signals at the YAC integration sites increased significantly (Fig. 6D,K,N). Therefore, prior chromosome breakage is not required for centromere chromatin reassembly at the alphoid YAC sites, and only the structural change of chromatin by hyperacetylation induced by TSA treatment is needed. No abnormalities were observed at the centromeres on host chromosomes after TSA treatment and no extra assembly of CENP-A, -B and -C was detected on the chromosome arm regions other than at the YAC integration site (Fig. 6G).

YAC integration sites derived from α21-II alphoid YAC (B13HT1) never formed minichromosomes after TSA treatment, nor did centromere components assemble there (Fig. 5C, Table 1), while transcription from the selectable marker gene increased (Fig. 5E). Thus, centromere component re-assembly occurs universally and specifically at the α21-I alphoid YAC/BAC integration sites of HT1080 cell lines. The centromere competence of the α21-II alphoid YAC integration site might be different from that of α21-I alphoid YAC integration sites, which show strong CENP-B binding.

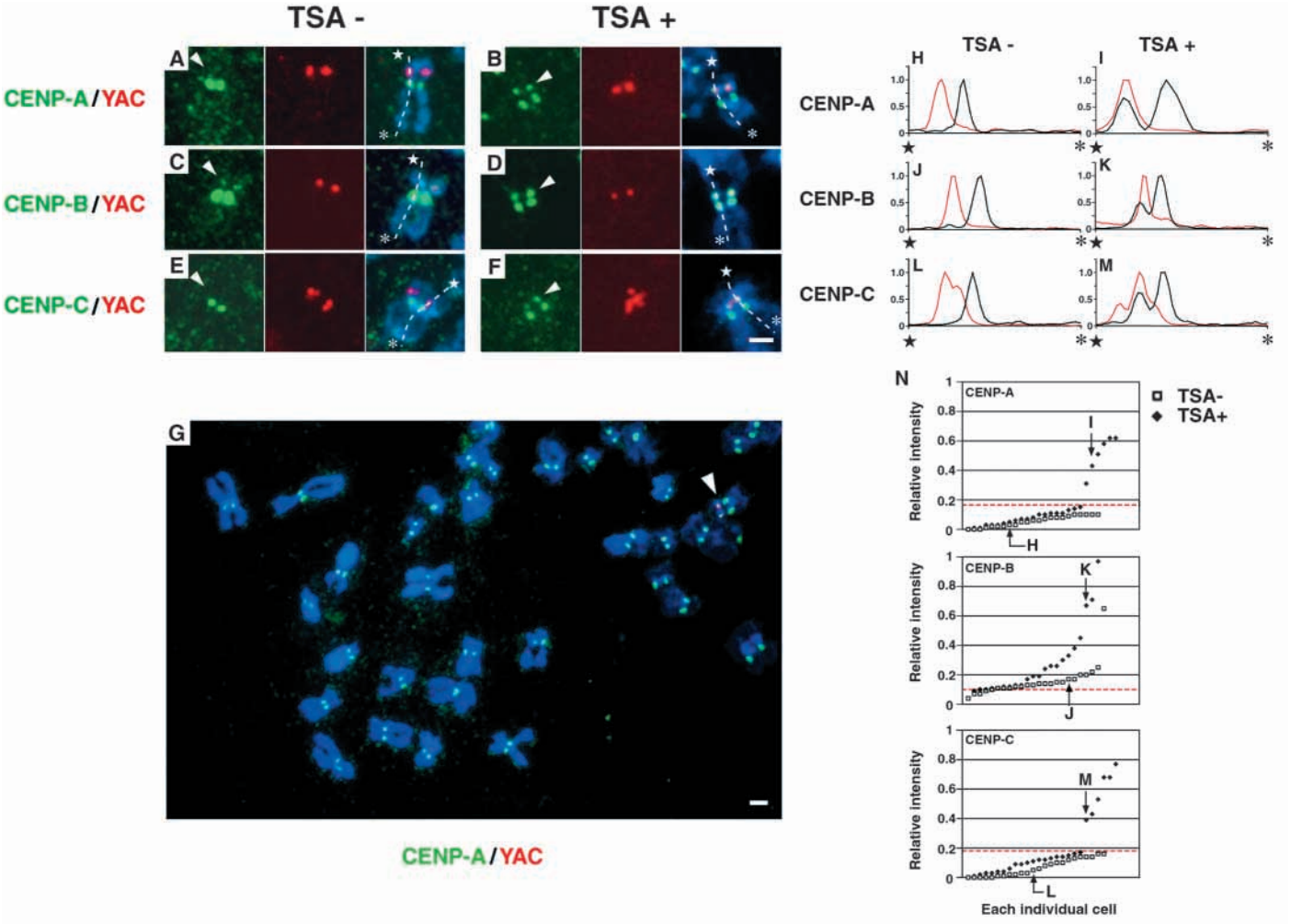

Fig. 6. De novo assembly of CENPs at the integrated 10 kb alphoid YAC DNA site without chromosome rearrangement. (A-G) Metaphase chromosomes from the del.22HT1-3 cell line, untreated (A,C,E) or treated (B,D,F,G) with 1000 ng/ml of TSA, analyzed by immunofluorescence using antibodies against CENPs (green), and FISH using the YAC arm probe (red). The chromosomes were counterstained with DAPI (blue). Arrowheads indicate the integration sites of the 10 kb alphoid YAC. Scale bars: 2 μm. (H-M) Intensity plot of CENP signals (black) and YAC signals (red) at the 10 kb alphoid YAC site on the host chromosome DNA. (N) The plots of relative intensity of CENP-A (upper), -B (middle), -C (lower) signals at each alphoid YAC integration site on the host centromeres in the del.22HT1-3 cell line untreated (square) or treated (diamond) with 1000 ng/ml of TSA. Red dotted lines indicate the lower limit of signals distinguishable from background levels.

Discussion

In many species, epigenetic controls of chromatin assembly including CENP-A appear to be fundamentally important in specifying the position of centromere structures and functions. However, the mechanisms and the molecular basis remain unclear. Our previous study showed that the information carried by the primary sequence of the α21-I alphoid DNA is important for de novo formation of functional centromere chromatin accompanied by binding of CENP-A, -B, -C and -E. Our present analyses indicate that epigenetic mechanisms also affect the centromere activity of α21-I alphoid YAC DNA at an ectopic locus. Two different cellular treatments, long-term culture under selection for a YAC marker and administration of TSA, which induced a change in chromatin structure, affected the assembly of CENPs at an ectopic alphoid YAC DNA site and caused the re-formation of minichromosomes with functional centromeres.

Centromere components assemble on 70 kb α21-I alphoid arrays but not on YAC arms in a stably propagated artificial chromosome

Our stable MACs consist of multimers of introduced α21-I alphoid YAC DNA. Cytological and ChIP analyses indicated that on a stable MAC with an active centromere, CENP-A and CENP-B assembled only on 70 kb α21-I alphoid arrays of the insert but not on sequences located 3 kb or 8 kb from the alphoid junctions on the YAC arms (Fig. 7A). CENP-A is also associated with neocentromeres. These findings suggest that assembly might not depend on specific DNA sequences (Lo et al., 2001). However, a DNA sequence underlying a neocentromere cannot undergo de novo centromere formation (Saffery et al., 2001). We have demonstrated that a synthetic alphoid construct with canonical CENP-B boxes is active for de novo centromere assembly including CENP-A, and can promote MAC formation, whereas the same construct with

point mutations affecting every CENP-B box does not exhibit these activities (Ohzeki et al., 2002). Thus, functional centromeres cannot form de novo on alphoid DNA without CENP-B boxes. Alphoid DNA with CENP-B boxes may have a specific capacity for assembling centromere chromatin.

In our present study, the *bsr* gene on the YAC arm was transcribed and acetylated histone H3 was assembled at this locus. Based on such an alphoid YAC multimer, a functional centromere structure was assembled and propagated as a stable MAC. Therefore, non-CENP-A chromatin intervals on the YAC arms between 70 kb alphoid repeats with CENP-A chromatin might not interrupt the functional kinetochore structures. These results might support the idea of a repeat subunit model of mammalian kinetochore at the molecular level (Zinkowski et al., 1991; Henikoff et al., 2000). Interestingly, interruption of CENP-A chromatin clusters with histone H3 chromatin was observed on the extended chromatin fiber of mitotic chromosomes in both human and *Drosophila* centromeres (Blower et al., 2002).

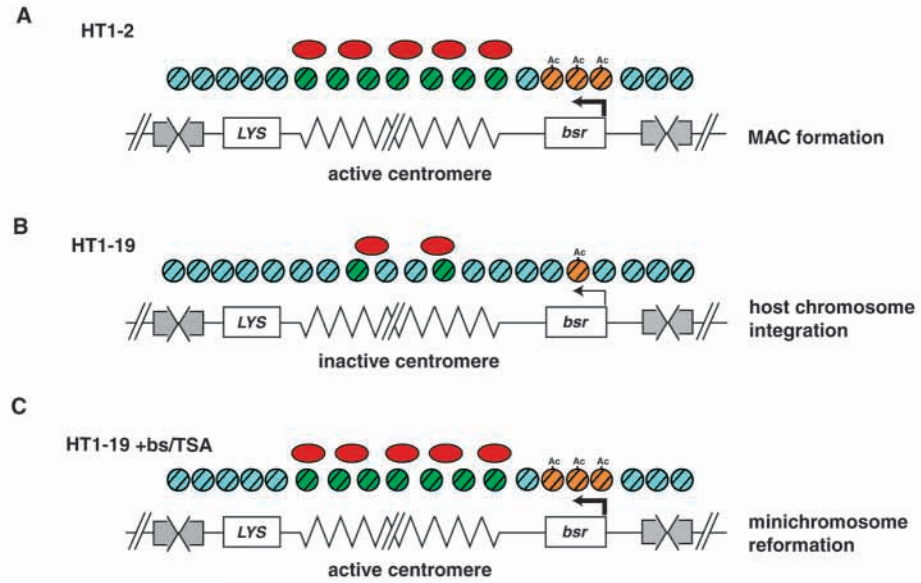

Fig. 7. Schematic representation of suppressed centromeres and functional centromere chromatin, and hypothetical models for the mechanism of assembly of centromere components on alphoid YAC. (A) On an artificial chromosome with a functional centromere/kinetochore structure, CENP-A and CENP-B assemble onto alphoid arrays in the introduced alphoid YAC DNA but not on YAC arms. *Bsr* genes on the YAC arms are transcribed, and histone H3 in chromatin on the genes is acetylated. (B) On the ectopic alphoid YAC loci, disassembly of centromere proteins from the insert alphoid arrays coincides with the reduction of the transcriptional activity from the *bsr* gene on the YAC arms and with the hypoacetylated level of histone H3 of the gene. (C) Increased gene expression on the YAC arms and hyperacetylation of histones by TSA causes structural change in chromatin at the integrated alphoid YAC DNA. Centromeric proteins can re-assemble at such regions and active centromeres re-form. Selection pressure might induce this process gradually during long-term culture.

Suppressed states of centromeres and reactivation at ectopic alphoid loci

At the site of integration of the alphoid YAC in 7C5HT1-19 cells the extent of CENP-A and -B assembly on the alphoid array was decreased compared with that on a stable MAC with an active centromere (Fig. 7B). These results, and the observation of the stability of the integrated alphoid YAC sequences at the same locus, indicated that centromere functions are lost or suppressed at the ectopic alphoid loci in this cell line, as in the inactive centromeres of dicentric chromosomes. Thus it is likely that a chromatin change makes the binding sites, including the CENP-B box, inaccessible. On the ectopic alphoid YAC loci, the transcription of *bsr* and the level of acetylated histone H3 on this gene also decreased (Fig. 7B). Therefore, not only was centromeric protein assembly inhibited, but many chromatin functions were also suppressed at the ectopic alphoid locus. At such suppressed (inactive) sites on the alphoid YAC loci, centromere chromatin was reassembled by long-term culture in selective medium. The results of TSA treatment also suggest that these reassemblies of components of the functional centromere/kinetochore structure were correlated with structural chromatin changes caused by histone acetylation, allowing a detectable increase in transcription of the nearby *bsr* gene to take place. We speculate that transcriptionally competent chromatin at the intervals between the 70 kb alphoid DNA arrays at the ectopic locations, or a hyperacetylated state of the histones due to TSA, would both be expected to break such a suppressed (inactivated) chromatin state at the loci by opening and remodeling the chromatin structure. Thus, one possible explanation for reassembly of centromere components is that the chromatin structure in the integrated suppressed alphoid DNA state might be changed by constant weak gene expression on the YAC arms or TSA-promoted hyperacetylation of histones as a common effect. CENPs and kinetochore proteins could be reassembled dependent on the capacity of open chromatin structure on α21-I alphoid YAC DNA even with the 10 kb alphoid insert, so that a functional centromere/kinetochore structure is re-formed (Fig. 7C). Alternatively, TSA may affect the transcription of genes that are presumed to contribute to centromere activation or centromeric protein assembly. However, as described below, several observations indicate that the latter possibility is incapable of explaining the reassembly phenomenon. BS selection, which has no relation to the transcription level of the endogenous presumptive centromere-related genes, also induces ectopic alphoid DNA activation to form a centromere. Centromere assembly on introduced α21-I alphoid DNA also occurred by selection of a nearby neomycin-resistance gene instead of the *bsr* gene (Ohzeki et al., 2002). Therefore, the former possibility is more likely: our analyses indicate that the

centromere activity of α21-I alphoid DNA at an ectopic locus can be altered as a result of changes in the chromatin structure of nearby genes.

Centromere activity and transcription

In fission yeast, components of the kinetochore, including yeast CENP-A, assemble on the central core of the centromere and the resulting complex is surrounded by heterochromatin (Saitoh et al., 1997; Takahashi et al., 2000; Partridge et al., 2000; Bernard et al., 2001; Nakagawa et al., 2002). TSA-induced high levels of transcription from genes inserted in centromeric flanking regions cause chromosome instability and conformational changes in centromeric heterochromatin (Ekwall et al., 1997). Moreover, the TSA-induced expression of the inserted genes was metastable and frequently reverted to a repressed state in the absence of TSA. This result suggests that functional centromeres, including heterochromatin regions, might be affected by changes in chromatin structure caused by strong transcriptional activity. However, in our experiment, TSA treatment has the opposite effect. In our system, marker gene transcription is regulated by the SV40 early promoter, which is not strong in this cell line (1/10-1/20 the level of that of the endogenous *β-actin* gene per 30 copies of YAC arms, as indicated by RT-PCR, Fig. 3F). This level of activity presumably suffices to allow the reassembly and maintenance of a functional centromere in our system. Strong transcriptional activity driven by the CMV and PGK promoter, however, drastically decreased the efficiency of artificial chromosome formation in our system (H. Nakashima and H.M., unpublished). Strong transcriptional activity or differences in chromatin structure as a result of the different promoter and enhancer between the 70 kb alphoid intervals may inhibit the active structure of centromeres or heterochromatin on artificial chromosomes. In both fission yeast and human cells, chromatin structures at the periphery of CENP-A-assembled core centromere domains affect centromere function (Nakagawa et al., 2002). In budding yeast, there is no evidence for epigenetical inactivation of the functional centromere, however, the phenotype of the *chl4* deletion mutant suggests that even in budding yeast, established centromeres are propagated in an epigenetic manner (Mythreye and Bloom, 2003). In addition, one centromere component, Cbf1, is a transcriptional regulator, and centromeric activity is also inhibited by strong transcription of genes inserted nearby (Bram and Kornberg, 1987; Hill and Bloom, 1987). Interestingly, Ams2, a GATA-type transcriptional regulator, is present in the central regions of fission yeast centromeres (Chen et al., 2003).

Centromere chromatin associated with pericentromeric heterochromatin

If endogenous centromere activity is affected positively or negatively by the chromatin structure that induces weak or strong transcription, chromosome loss and breakage leading to severe aneuploidy might be caused. Conversely, centromeric chromatin structure might inhibit transcriptional regulation of flanking genes. Therefore, to stabilize centromere activity it would be reasonable to place centromeres in specific chromosomal regions away from transcriptional activities. Indeed, normal human centromeres are located on megabase-sized alphoid arrays in normal human cells. Furthermore, the long alphoid arrays in endogenous chromosomes are surrounded by large regions of inactive heterochromatin. In mouse and *Drosophila* centromeres, large tracts of pericentromeric heterochromatin are also observed adjacent to centromeric satellite DNAs on which CENPs assemble (Mitchell et al., 1993; Blower and Karpen, 2001). It is possible that the structure of endogenous centromeres is protected by pericentromeric heterochromatin (Choo, 2001). Even when the cells were treated with TSA, which induced the reactivation of suppressed centromeres in the integrated alphoid YAC, endogenous centromeres did not exhibit abnormalities in centromere component assembly. Our results also indicated that CENP-A might not be acetylated by treatment with TSA. Thus, once assembled, CENP-A chromatin may be more TSA-resistant or -insensitive than histone H3 chromatin. The findings of Taddei et al. supports this: TSA treatment was found to cause the disassembly of HP1 from regions of pericentromeric heterochromatin but did not impair centromeric protein assembly (Taddei et al., 2001).

Assembly of the centromeric proteins CENP-A and CENP-C into chromatin was observed in a limited area on the MACs, whereas CENP-B was detected almost throughout the MACs, so that not all the alphoid DNA arrays in the approx. 30 copies of introduced alphoid YAC DNA might be involved in kinetochore assembly. The remainder of the alphoid array on the multimerized YAC DNA might be important for the formation of structures other than the kinetochore, such as pericentromeric heterochromatin or other states of chromatin such as a stable artificial chromosome. Actually, anti-CENP-A antibodies have been reported to stain only one-half to two-thirds of the alphoid regions of normal human centromeres analyzed by fiber FISH (Blower et al., 2002). In fission yeast, pericentromeric heterochromatin is involved in sister chromatid cohesion (Bernard et al., 2001; Nonaka et al., 2002).

A more detailed understanding of centromere assembly will require further investigation of centromere structure and function with respect to protein assembly, epigenetic modifications of histones, and DNA modifications (such as methylation), as well as the organization of heterochromatin. Our alphoid YAC construct integrated into ectopic chromosomal locations will provide a powerful tool not only for the analysis of artificial chromosomes, but also for the generation of novel views of the functional organization of centromeres, heterochromatin and chromosomes in mammals, which are very difficult to analyze.

We thank K. Yoda (Nagoya University) for producing the anti-CENP-A antibody, N. Nozaki (Kanagawa Dental College) for producing anti-CENP-A and -B antibodies, K. Ohta (Genetic Dynamics Research Unit-Laboratory, RIKEN) for sharing the method of cell fixation for ChIP analysis, Prof. A. Sugino for many helpful discussions, T. Higuchi (CREST) for technical assistance, M. Hirano for secretarial work and M. Ikeno (Fujita Health University) for technical discussion. This work was supported by a grant-in-aid for Scientific Research on Priority Areas (B), Core Research for Evolutional Science and Technology (CREST), and Special Coordination Funds for Promoting Science and Technology from the Ministry of Education, Science, Sports and Culture of Japan, a grant-in-aid for Basic Research 21 for Breakthroughs in Info-

Communications and a grant-in-aid from the Cell Science Research Foundation.

References

Bartsch, J., Truss, M., Bode, J. and Beato, M. (1996). Moderate increase in histone acetylation activates the mouse mammary tumor virus promoter and remodels its nucleosome structure. *Proc. Natl. Acad. Sci. USA* **93**, 10741-10746.

Bernard, P., Maure, J. F., Partridge, J. F., Genier, S., Javerzat, J. P. and Allshire, R. C. (2001). Requirement of heterochromatin for cohesin at centromeres. *Science* **294**, 2539-2542.

Blower, M. D. and Karpen, G. H. (2001). The role of Drosophila CID in kinetochore formation, cell-cycle progression and heterochromatin interactions. *Nature Cell Biol.* **3**, 730-739.

Blower, M. D., Sullivan, B. A. and Karpen G. H. (2002). Conserved organization of centromeric chromatin in flies and humans. *Dev. Cell* **2**, 319-330.

Bram, R. J. and Kornberg, R. D. (1987). Isolation of a Saccharomyces cerevisiae centromere DNA-binding protein, its human homolog, and its possible role as a transcription factor. *Mol. Cell. Biol.* **7**, 403-409.

Brinkley, B. R. and Stubblefield, E. (1966). The fine structure of the kinetochore of a mammalian cell in vitro. *Chromosoma* **19**, 28-43.

Burke, D. T., Carle, G. F. and Olson, M. V. (1987). Cloning of large segments of exogenous DNA into yeast by means of artificial chromosome vectors. *Science* **236**, 806-812.

Candido, E. P., Reeves, R. and Davie, J. R. (1978). Sodium butyrate inhibits histone deacetylation in cultured cells. *Cell* **14**, 105-113.

Chen, E. S., Saitoh, S., Yanagida, M. and Takahashi, K. (2003). A cell cycle-regulated GATA factor promotes centromeric localization of CENP-A in fission yeast. *Mol. Cell* **11**, 175-187.

Choo, K. H., Vissel, B., Nagy, A., Earle, E. and Kalitsis, P. (1991). A survey of the genomic distribution of alpha satellite DNA on all the human chromosomes, and derivation of a new consensus sequence. *Nucleic Acids Res.* **19**, 1179-1182.

Choo, K. H. (2001). Domain organization at the centromere and neocentromere. *Dev. Cell* **1**, 165-177.

Cleveland, D. W., Mao, Y. and Sullivan, K. F. (2003). Centromeres and kinetochores: From epigenetics to mitotic checkpoint signaling. *Cell* **112**, 407-421.

Cooke, C. A., Bernat, R. L. and Earnshaw, W. C. (1990). CENP-B: a major human centromere protein located beneath the kinetochore. *J. Cell Biol.* **110**, 1475-1488.

Dinos, G. P. and Kalpaxis, D. L. (1997). Heat and ionic limitations do not change the inhibition pattern of ribosomal peptidyltransferase by aminohexosyl-cytosine nucleoside antibiotics. *Pharmazie* **52**, 875-877.

du Sart, D., Cancilla, M. R., Earle, E., Mao, J. I., Saffery, R., Tainton, K. M., Kalitsis, P., Martyn, J., Barry, A. E. and Choo, K. H. (1997). A functional neo-centromere formed through activation of a latent human centromere and consisting of non-alpha-satellite DNA. *Nat. Genet.* **16**, 144-153.

Earnshaw, W. C. and Migeon, B. R. (1985). Three related centromere proteins are absent from the inactive centromere of a stable isodicentric chromosome. *Chromosoma* **92**, 290-296.

Earnshaw, W. C., Sullivan, K. F., Machlin, P. S., Cooke, C. A., Kaiser, D. A., Pollard, T. D., Rothfield, N. F. and Cleveland, D. W. (1987). Molecular cloning of cDNA for CENP-B, the major human centromere autoantigen. *J. Cell Biol.* **104**, 817-829.

Ebersole, T. A., Ross, A., Clark, E., McGill, N., Schindelhauer, D., Cooke, H. and Grimes, B. (2000). Mammalian artificial chromosome formation from circular alphoid input DNA does not require telomere repeats. *Hum. Mol. Genet.* **9**, 1623-1631.

Ekwall, K., Olsson, T., Turner, B. M., Cranston, G. and Allshire, R. C. (1997). Transient inhibition of histone deacetylation alters the structural and functional imprint at fission yeast centromeres. *Cell* **91**, 1021-1032.

Fisher, A. M., Al-Gazali, L., Pramathan, T., Quaife, R., Cockwell, A. E., Barber, J. C., Earnshaw, W. C., Axelman, J., Migeon, B. R. and Tyler-Smith, C. (1997). Centromeric inactivation in a dicentric human Y;21 translocation chromosome. *Chromosoma* **106**, 199-206.

Goshima, G., Kiyomitsu, T., Yoda, K. and Yanagida, M. (2003). Human centromere chromatin protein hMis12, essential for equal segregation, is independent of CENP-A loading pathway. *J. Cell Biol.* **160**, 25-39.

Grimes, B. R., Rhoades, A. A. and Willard, H. F. (2002). Alpha-satellite DNA and vector composition influence rates of human artificial chromosome formation. *Mol. Ther.* **5**, 798-805.

Harrington, J. J., van Bokkelen, G., Mays, R. W., Gustashaw, K. and Willard, H. F. (1997). Formation of de novo centromeres and construction of first-generation human artificial microchromosomes. *Nat. Genet.* **15**, 345-355.

Henikoff, S., Ahmad, K., Platero, J. S. and van Steensel, B. (2000). Heterochromatic deposition of centromeric histone H3-like proteins. *Proc. Natl. Acad. Sci. USA* **97**, 716-721.

Henikoff, S., Ahmad, K. and Malik, H. S. (2001). The centromere paradox: stable inheritance with rapidly evolving DNA. *Science* **293**, 1098-1102.

Henning, K. A., Novotny, E. A., Compton, S. T., Guan, X. Y., Liu, P. P. and Ashlock, M. A. (1999). Human artificial chromosomes generated by modification of a yeast artificial chromosome containing both human alpha satellite and single-copy DNA sequences. *Proc. Natl. Acad. Sci. USA* **96**, 592-597.

Hill, A. and Bloom, K. (1987). Genetic manipulation of centromere function. *Mol. Cell. Biol.* **7**, 2397-2405.

Holt, S. E., Wright, W. E. and Shay, J. W. (1996). Regulation of telomerase activity in immortal cell lines. *Mol. Cell. Biol.* **16**, 2932-2939

Ikeno, M., Masumoto, H. and Okazaki, T. (1994). Distribution of CENP-B boxes reflected in CREST centromere antigenic sites on long-range α-satellite DNA arrays of human chromosome 21. *Hum. Mol. Genet.* **3**, 1245-1257.

Ikeno, M., Grimes, B., Okazaki, T., Nakano, M., Saitoh, K., Hoshino, H., McGill, N. I., Cooke, H. and Masumoto, H. (1998). Construction of YAC-based mammalian artificial chromosomes. *Nat. Biotechnol.* **16**, 431-439.

Kitagawa, K. and Hieter, P. (2001). Evolutionary conservation between budding yeast and human kinetochores. *Nat. Rev. Mol. Cell. Biol.* **2**, 678-687.

Liu, S. T., Hittle, J. C., Jablonski, S. A., Campbell, M. S., Yoda, K. and Yen, T. J. (2003). Human CENP-I specifies localization of CENP-F, MAD1 and MAD2 to kinetochores and is essential for mitosis. *Nature Cell Biol.* **5**, 341-345.

Lo, A. W., Craig, J. M., Saffery, R., Kalitsis, P., Irvine, D.V., Earle, E., Magliano, D. J. and Choo, K. H. (2001). A 330 kb CENP-A binding domain and altered replication timing at a human neocentromere. *EMBO J.* **20**, 2087-2096.

Marcais, B., Laurent, A. M., Charlieu, J. P. and Roizes, G. (1993). Organization of the variant domains of alpha satellite DNA on human chromosome 21. *J. Mol. Evol.* **37**, 171-178.

Masumoto, H., Sugimoto, K. and Okazaki, T. (1989a). Alphoid satellite DNA is tightly associated with centromere antigens in human chromosomes throughout the cell cycle. *Exp. Cell Res.* **181**, 181-196.

Masumoto, H., Masukata, H., Muro, Y., Nozaki, N. and Okazaki, T. (1989b). A human centromere antigen (CENP-B) interacts with a short specific sequence in alphoid DNA, a human centromeric satellite. *J. Cell Biol.* **109**, 1963-1973.

Masumoto, H., Ikeno, M., Nakano, M., Okazaki, T., Grimes, B., Cooke, H. and Suzuki, N. (1998). Assay of centromere function using a human artificial chromosome. *Chromosoma* **107**, 406-416.

Mejia, J. E., Willmott, A., Levy, E., Earnshaw, W. C. and Larin, Z. (2001). Functional complementation of a genetic deficiency with human artificial chromosomes. *Am. J. Hum. Genet.* **69**, 315-326.

Mitchell, A. R., Nicol, L., Malloy, P. and Kipling, D. (1993). Novel structural organization of a Mus musculus DBA/2 chromosome shows a fixed position for the centromere. *J. Cell Sci.* **106**, 79-85.

Murphy, T. D. and Karpen, G. F. (1998). Centromeres take flight: alpha satellite and the quest for the human centromere. *Cell* **93**, 317-320.

Mythreye, K. and Bloom, K. S. (2003). Differential kinetochore protein requirements for establishment versus propagation of centromere activity in *Saccharomyces cerevisiae*. *J. Cell Biol.* **160**, 833-843.

Nakagawa, H., Lee, J. K., Hurwitz, J., Allshire, R. C., Nakayama, J., Grewal, S. I., Tanaka, K. and Murakami, Y. (2002). Fission yeast CENP-B homologs nucleate centromeric heterochromatin by promoting heterochromatin-specific histone tail modifications. *Genes Dev.* **16**, 1766-1778.

Nonaka, N., Kitajima, T., Yokobayashi, S., Xiao, G., Yamamoto, M., Grewal, S. I. and Watanabe, Y. (2002). Recruitment of cohesin to heterochromatic regions by Swi6/HP1 in fission yeast. *Nat. Cell Biol.* **4**, 89-93.

Ohzeki, J., Nakano, M., Okada, T. and Masumoto, H. (2002). CENP-B box

is required for de novo centromere chromatin assembly on human alphoid DNA. *J. Cell Biol.* **159**, 765-775.

Palmer, D. K., O'Day, K., Trong, H. L., Charbonneau, H. and Margolis, R. L. (1991). Purification of the centromere-specific protein CENP-A and demonstration that it is a distinctive histone. *Proc. Natl. Acad. Sci. USA* **88**, 3734-3738.

Partridge, J. F., Borgstrom, B. and Allshire, R. C. (2000). Distinct protein interaction domains and protein spreading in a complex centromere. *Genes Dev.* **14**, 783-791.

Pluta, A. F., Mackay, A. M., Ainsztein, A. M., Goldberg, I. G. and Earnshaw, W. C. (1995). The centromere: hub of chromosomal activities. *Science* **270**, 1591-1594.

Rattner, J. B. (1987). The organization of the mammalian kinetochore: a scanning electron microscope study. *Chromosoma* **95**, 175-181.

Saffery, R., Irvine, D. V., Griffiths, B., Kalitsis, P., Wordeman, L. and Choo, K. H. (2000). Human centromeres and neocentromeres show identical distribution patterns of >20 functionally important kinetochore-associated proteins. *Hum. Mol. Genet.* **9**, 175-185.

Saffery, R., Wong, L. H., Irvine, D. V., Beteman, M. A., Griffiths, B., Cuttes, S. M., Cancilla, M. R., Cendron, A. C., Stafford, A. J. and Choo, K. H. (2001). Construction of neocentromere-based human minichromosomes by telomere-associated chromosomal truncation. *Proc. Natl. Acad. Sci. USA* **98**, 5705-5710.

Saitoh, H., Tomkiel, J., Cooke, C. A., Ratrie, H., III, Maurer, M., Rothfield, N. F. and Earnshaw, W. C. (1992). CENP-C, an autoantigen in scleroderma, is a component of the human inner kinetochore plate. *Cell* **70**, 115-125.

Saitoh, S., Takahashi, K. and Yanagida, M. (1997). Mis6, a fission yeast inner centromere protein, acts during G1/S and forms specialized chromatin required for equal segregation. *Cell* **90**, 131-143.

Shelby, R. D., Monier, K. and Sullivan, K. F. (2000). Chromatin assembly at kinetochores is uncoupled from DNA replication. *J. Cell Biol.* **151**, 1113-1118.

Steiner, N. C. and Clarke, L. (1994). A novel epigenetic effect can alter centromere function in fission yeast. *Cell* **79**, 865-874.

Sullivan, B. A. and Schwartz, S. (1995). Identification of centromeric antigens in dicentric Robertsonian translocations: CENP-C and CENP-E are necessary components of functional centromeres. *Hum. Mol. Genet.* **4**, 2189-2197.

Sullivan, K. F., Hechenberger, M. and Masri, K. (1994). Human CENP-A contains a histone H3 related histone fold domain that is required for targeting to the centromere. *J. Cell Biol.* **127**, 581-592.

Taddei, A., Maison, C., Roche, D. and Almouzni, G. (2001). Reversible disruption of pericentric heterochromatin and centromere function by inhibiting deacetylases. *Nat. Cell Biol.* **3**, 114-120.

Takahashi, K., Chen, E. S. and Yanagida, M. (2000). Requirement of Mis6 centromere connector for localizing a CENP-A-like protein in fission yeast. *Science* **288**, 2215-2219.

Tsutsui, T., Kumakura, S., Tamura, Y., Tsutsui, T., Sekiguchi, M., Higuchi, T. and Barrett, J. C. (2003). Immortal, telomerase-negative cell lines derived from a Li-Fraumeni syndrome patient exhibit telomere length variability and chromosomal and minisatellite instabilities. *Carcinogenesis* **24**, 953-965.

Warburton, P. E., Cooke, C. A., Bourassa, S., Vafa, O., Sullivan, B. A., Stetten, G., Gimelli, G., Warburton, D., Tyler-Smith, C., Sullivan, K. F. et al. (1997). Immunolocalization of CENP-A suggests a distinct nucleosome structure at the inner kinetochore plate of active centromeres. *Curr. Biol.* **7**, 901-904.

Warburton, P. E. (2001). Epigenetic analysis of kinetochore assembly on variant human centromeres. *Trends Genet.* **17**, 243-247.

Wiens, G. R. and Sorger, P. K. (1998). Centromeric chromatin and epigenetic effects in kinetochore assembly. *Cell* **93**, 313-316.

Willard, H. F. and Waye, J. S. (1987). Hierarchical order in chromosome-specific human alpha satellite DNA. *Trends Genet.* **3**, 192-198.

Williams, B. C., Murphy, T. D., Goldberg, M. L. and Karpen, G. H. (1998). Neocentromere activity of structurally acentric mini-chromosomes in Drosophila. *Nat. Genet.* **18**, 30-37.

Wood, K. W., Sakowicz, R., Goldstein, L. S. and Cleveland, D. W. (1997). CENP-E is a plus end-directed kinetochore motor required for metaphase chromosome alignment. *Cell* **91**, 357-366.

Yen, T. J., Compton, D. A., Wise, D., Zinkowski, R. P., Brinkley, B. R., Earnshaw, W. C. and Cleveland, D. W. (1991). CENP-E, a novel human centromere-associated protein required for progression from metaphase to anaphase. *EMBO J.* **10**, 1245-1254.

Yoshida, M., Kijima, M., Akita, M. and Beppu, T. (1990). Potent and specific inhibition of mammalian histone deacetylase both in vivo and in vitro by trichostatin A. *J. Biol. Chem.* **265**, 17174-17179.

Zinkowski, R. P., Meyne, J. and Brinkley, B. R. (1991). The centromere-kinetochore complex: a repeat subunit model. *J. Cell Biol.* **113**, 1091-1110.